ETA-II BEAM BRIGHTNESS MEASUREMENT*

A.C.Paul, S.L.Allen, F.W.Chambers, Y-J.Chen, F.J.Deadrick, W.C.Turner
Lawrence Livermore National Laboratory
P.O.Box 808, L626, Livermore, California, 94550

Abstract - ETA-II resumed operation in the Fall of 1990 with the injector and first two 10 cell accelerating blocks and nominal electron beam parameters of 1500 Amperes, 2.5 MeV, 70 nsec pulse width at 1 Hz PRF. The beam brightness diagnostics consisted of a Cherenkov foil view port and a pepper-pot emittance diagnostic. The Cherenkov foil experiment was used to determine the beam energy at the accelerator exit. The pepper-pot emittance diagnostic was used to determine the whole beam brightness. The brightness as a function of beam radius and time within the beam pulse was also measured. The brightness is defined as the ratio of the beam current within a given radius to the normalized four dimensional volume occupied by particles within that radius.

1. Emittance techniques

At ETA II we have used several techniques to measure the beam emittance and hence the beam brightness; 1) the two hole emittance diagnostic (TSES), [1] 2) solenoidal magnet field versus beam radius scans using Cherenkov foil light, [2] and 3) pepper-pot emittance diagnostic (PPED) using a mask and its down stream image. The TSES measures only the local beam emittance at the location of the first hole and as such does not give a whole beam measurement. For the expected operational parameters of ETA II in this low-energy space-charge dominated regime, the Cherenkov foil scan technique would be marginal for determining the whole beam emittance. For these reasons, we selected the PPED in the experiments reported here. The nominal ETA II operational parameters are expected to give a beam brightness, J, in the range $1\times10^8 < J < 1\times10^{10}$ A/(m–rad)^2.

2. Pepper-pot emittance measurement

The pepper-pot diagnostic mask consists of a range-thick array of 0.05 cm diameter holes, spaced 0.7 cm, on a square 11 by 11 pattern. The beam incident on the mask is transmitted as a number of beamlets 80 cm down stream to a view phosphor. We measure the beam current incident on the mask, I_{B4}, and the total transmitted current, I_{T3}. The image is digitally recorded with a gated TV camera and a 512 by 480 pixel frame grabber, fig.1[1]. The time gate is adjustable and typically set to 5-10 nsec. The gate can be "walked" through the beam pulse to obtain a measurement along the 40 nsec beam flat top. The emittance of each beamlet is obtained from the expansion of the beamlet observed at the phosphor from the known beamlet size at the mask.

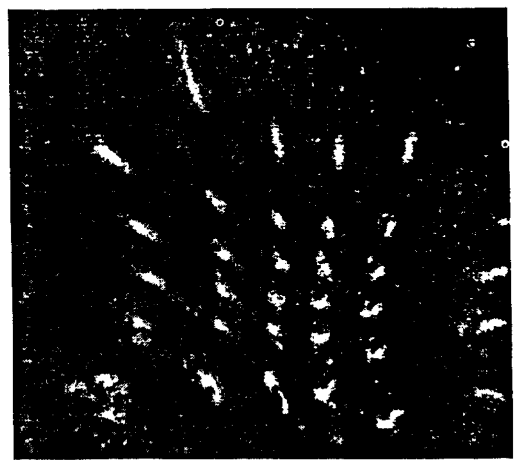

Figure 1. TV pepper-pot image showing 33 beamlets. A current of 1321 Amperes impinged on the mask, 4.72 Amperes passed to the phosphor (R0339F11.RAS).

In this work, we make no assumption about the beam being at a waist at the pepper-pot mask. We do assume the beam size at the mask, R, is large relative to the mask hole radii, r_h, fig.2. Let x_n be the measured half size of beamlet n. The angular divergence (expansion) of a beamlet in a drift of length L is given by

$$x_n' = \frac{x_n - r_h}{L} \quad . \qquad [1]$$

The horizontal hard edge beam emittance is calculated from the beamlet statistical averages as

$$<x^2> \equiv \sum_{n=1}^{n=2N_b} x_n^2 \;, \quad <x'^2> \equiv \sum_{n=1}^{n=2N_b} x'^2_n \;, \quad <x\,x'> \equiv \sum_{n=1}^{n=2N_b} x_n\, x'_n \qquad [2]$$

N_b being the total number of beamlets passed by the mask. Each beamlet contributes two points two these averages, x_o, x_1' and x_o, x_2', the beamlet extremals, fig.2. The beam

* This work was performed jointly under the auspices of the US Department of Energy by Lawrence Livermore National Laboratory under W-7405-ENG-48 and for the department of Defense under SDIO/SDC MIPR No. W31RPD-8-D5005.

[1] All figures in this paper were done with user friendly IDL graphics. *"IDL, Interactive Data Language"* Research Systems, Inc. 2021 Albion St. Denver, CO 80207

emittance given by the hard edge σ matrix representing the coefficients of the ellipse bounding all points of the beamlets[2],

$$\varepsilon_x^2 \equiv \sigma_{11}\sigma_{22} - \sigma_{12}^2 \quad [3]$$

$$= \frac{4}{N_b^2}\left[<x^2><x'^2> - <x\,x'>^2\right] \ . \quad [4]$$

Analogously in the vertical plane

$$\varepsilon_y^2 \equiv \sigma_{33}\sigma_{44} - \sigma_{34}^2 \quad [5]$$

$$= \frac{4}{N_b^2}\left[<y^2><y'^2> - <y\,y'>^2\right] \ . \quad [6]$$

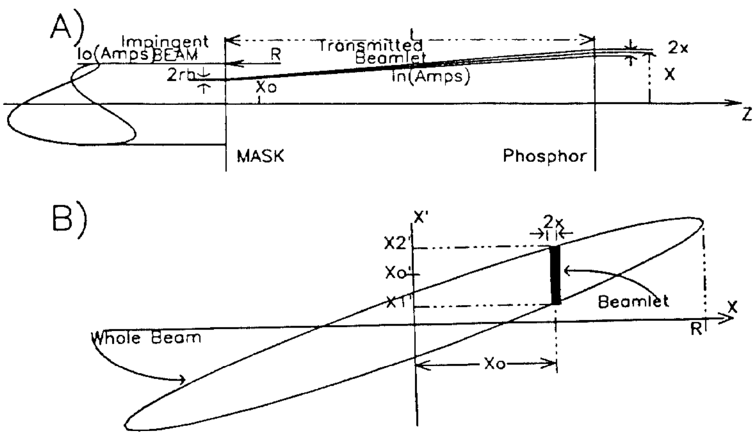

Figure 2. Pepper-pot geometry showing A) one typical beamlet, B) phase space of whole beam and beamlet at location of the mask.

At the mask, the beamlet of width $2r_h$ and angular divergence $2x_n'$ has a phase space centroid location at (X_o, X_o') :

$$X_o' = \frac{X - X_o}{L} \ , \quad [7]$$

where X is the absolute location of the beamlet of width $2x_n$ at the image and X_o is the x value of the mask hole center through which this beamlet has passed.

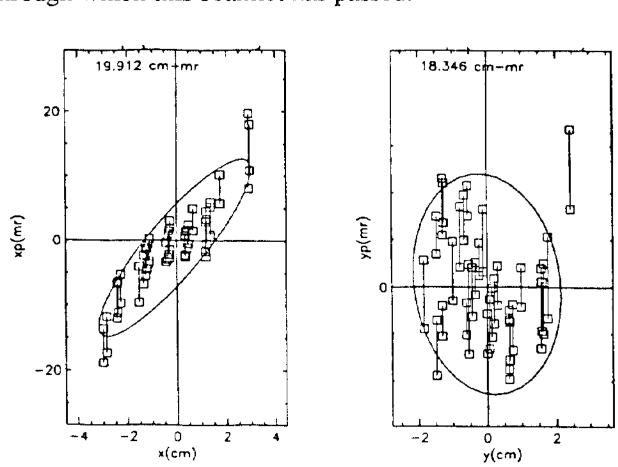

Figure 3. x-x' and y-y' phase space unfolding from expansion of beamlets for R0339F11.RAS, table 2.

[2] Note that each < > term as a factor of 2 from the sums, eq.[2] n=1.. $2N_b$, hence $\varepsilon_{x,y} = 4\,\varepsilon_{rms}$ as usual.

The elliptical contour bounding all of the beamlets may have a larger angular extent than the individual beamlets due to the inclusion of the relative beamlet-to-beamlet divergence, fig.3. This divergence can be caused by aberrations, canonical momentum from magnetic field threading the cathode, or other sources.

3. Brightness

The brightness of the n[th] individual beamlet is

$$j_n = \frac{i_n}{(\pi\,\beta\gamma\,r_h\,\theta_n)^2} \ , \quad [8]$$

θ_n is the angular divergence of the n-th beamlet, $i_n = I_{pass}\sum pixel_n/\sum pixels_{all}$ with I_{pass} taken either as the measured passed current I_{T3} or the calculated geometric current $I_{B4}\,N_b(r_h/R)^2$. The average brightness of all the beamlets is

$$J_{ave} = \frac{1}{N_b}\sum j_n \ . \quad [9]$$

The whole beam brightness, J_{xy} , based on the four dimensional elliptical volume, $\pi^2\varepsilon_x\varepsilon_y/2$, is

$$J_{xy} = \frac{2\,I_{B4}}{(\pi\,\beta\gamma)^2\,\varepsilon_x\varepsilon_y} \ . \quad [10]$$

If there is no phase space distortion and we correctly measure the beam radius and current impingent on the mask and the current passed by the mask, then the whole beam and average beamlet brightness would be the same. The intrinsic brightness of the beamlets can differ from the whole beam brightness by the degradations introduced by whatever whole beam phase space distortions are present.

4. Beam energy

The value of $\beta\gamma$ used in the brightness calculation was obtained from a scan of the observed beam radius versus field of the last six focusing magnets at the end of the accelerator. Consider the beam envelope equation for a section of solenoid transport including both the emittance and space charge terms:

$$r'' + k^2 r = \frac{\varepsilon^2}{r^3} + \frac{2\,I}{I_a(\beta\gamma)^3}\,\frac{1}{r} \ , \quad [11]$$

with $k = B/2(B\rho)$, $I_a = 4\pi\varepsilon_o c E_o$, E_o the beam rest energy in Volts. For electrons, I_a is 17000 Amperes. Expanding the radius, $r = r_o + a$, about the matched value r_o gives the small amplitude perturbed motion

$$a'' + 2\left[\frac{\varepsilon^2}{r_o^4} + k^2\right] a = 0 \quad [12]$$

whose solution is

$$a = a_o \sin\left[\sqrt{2}\left[\frac{\varepsilon^2}{r_o^4} + k^2\right]^{1/2} z\right] \ . \quad [13]$$

The minima occur at multiples of π . Let the number of oscillations the beam has undergone at the first minima be n. Then the number of oscillations at the second minima is $(n+1)\pi$ etc. The positions of the first, second, ... minima of the observed beam oscillations allow a solution for the value of $\beta\gamma$ by eliminating n from the above equations:

$$\beta\gamma=\frac{\Lambda}{\sqrt{2}\,\pi}\left[\left[\frac{B_2^2}{(E_o/ec)^2}+\frac{4\varepsilon_n^2}{r_o^4}\right]^{1/2}-\left[\frac{B_1^2}{(E_o/ec)^2}+\frac{4\varepsilon_n^2}{r_o^4}\right]^{1/2}\right] \quad [14]$$

B_1, B_2 being the field value at the first and second minima, Λ the length of the solenoid section, and ε_n the normalized emittance. $\beta\gamma$ is the average value inside the section of accelerator that is scanned. The final beam energy at the end of the machine will be higher by the additional acceleration produced by the last three accelerating gaps. The final beam energy compares favorably with the value deduced from reference [3].

Table 1.

Minima	Solenoid Amperes	Field kG	$\beta\gamma$ -3 gaps	E(final) MeV
B_1	73	0.489		
B_2	126	0.845	5.394	2.547
B_3	172	1.153	5.541	2.621

5. Summary of ETA-II pepper-pot beam brightness

A summary of ETA-II beam brightness for pepper-pot hole patterns of 4X4 to 11X11 with both crossover and no crossover between the mask and the view phosphor is given in table 2, below. For the beam of figures 1 and 3 the brightness is shown in fig.4.

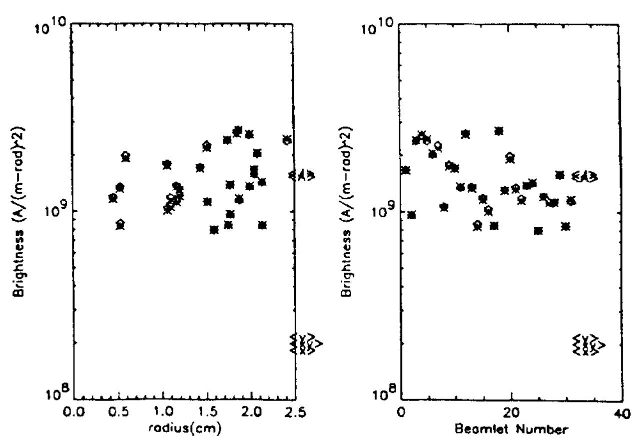

Figure 4. Brightness of beamlets of figure 1 at the location of the mask. <A> is the average of the beamlets, <xy> is the whole beam value.

Much of the scatter in brightness between the individual beamlets has resulted from the difference in the x and y emittance resulting from the elliptical shape of the image. This elliptical shape has resulted from scattering of the beamlet on passage through the mask. The brightness has been measured for 10 nsec time slots spaced every 5 nsec through the beam pulse flat top. The brightness is not a strong function of the time after correction has been made for the variation of beam energy and loading.

Table 2.

Image	I_{B4} Amps	I_{T3} Amps	N_b	J_{ave} A/(m−rad)^2	J_{xy} A/(m−rad)^2
309f07	1453	2.24	15	2.07×10^9	3.44×10^8
310f0e	1181	1.70	16	1.65×10^9	(4)
324f01	1400	25	90	1.88×10^9	2.66×10^8
333f0b	1000	3.00	110	7.69×10^8	4.16×10^8
339f1i	846	2.93	39	2.24×10^9	1.96×10^8
339f11	1321	4.72	33	1.82×10^9	2.22×10^8
341f02	1000	3.79	23	2.82×10^9	2.74×10^8
341f07	1392	4.50	33	1.68×10^9	3.60×10^8

6. Conclusions

The intrinsic beamlet brightness ($1–4\times10^9$) is about an order of magnitude higher than the observed whole beam brightness ($1–3\times10^8$). The brightness of the cathode has been previously studied [6] and is 1×10^{10} . The source of the degradation of the beam brightness is under investigation [4]. For the upcoming FEL experiments the present whole beam brightness is satisfactory. Correction for space charge and the ellipticity of the beamlet images introduced by scattering in passing through the mask will increase the beam brightness. Space charge corrections increase the brightness by about 20%. The correction for beamlet ellipticity reduces the beamlet to beamlet scatter evident in fig.4 and increases the intrinsic beamlet brightness by something less than a factor of two. These corrections to the analysis are currently being implemented.

References

[1] W. E. Nexsen et.al., "The ETA-II Induction Linac as a High-Average-Power FEL Drive," *Nuclear Instruments and Methods,* NIM-A296(1990)54-61

[2] A. C. Paul et.al., "Probing the Electron Distribution Inside the ATA Beam Pulse," *Nuclear Instruments and Methods,* NIM-A300(1991)137-150

[3] W. E. Nexsen et.al.,"Reduction of Energy Sweep of the ETA-II Beam," *Paper this conference*

[4] Y-J. Chen et.al.,"Degradation of Brightness by Resonant Particle Effects," *Paper this conference*

[5] W.C. Turner, et.al.,"High-Brightness, High-Current Density Cathode for Induction Linac FELs," 1988 Linear Accelerator Conference, Williamsburg, Virginia, Oct 2-7, 1988.

[6] W.C. Turner, et.al.,"Status of the ETA-II Linear Induction Accelerator - High Brightness Results," 1989 Particle Accelerator Conference, Chicago, Illinois, March 20-23, 1989.

[4] The whole beam value of 1.04×10^9 was for a measured I_{T3} current of 1.70 Amperes. The expected transmitted current was 5.4 Amperes.